

Sea level along the world's coastlines can be measured by a network of virtual altimetry stations

Anny Cazenave¹✉, Yvan Gouzenes¹, Florence Birol¹, Fabien Leger¹, Marcello Passaro², Francisco M. Calafat³, Andrew Shaw⁴, Fernando Nino¹, Jean François Legeais⁵, Julius Oelsmann², Marco Restano⁶ & Jérôme Benveniste⁷

For nearly 30 years, space-based radar altimetry has been routinely measuring changes in sea level at global and regional scales. But this technique designed for the open ocean does not provide reliable sea level data within 20 km to the coast, mostly due to land contamination within the radar echo in the vicinity of the coast. This problem can now be overcome through dedicated reprocessing, allowing the retrieval of valid sea level data in the 0–20 km band from the coast, and then the access to novel information on sea level change in the world coastal zones. Here we present sea level anomalies and associated coastal sea level trends at 756 altimetry-based virtual coastal stations located along the coasts of North and South America, Northeast Atlantic, Mediterranean Sea, Africa, North Indian Ocean, Asia and Australia. This new dataset, derived from the reprocessing of high-resolution (300 m) along-track altimetry data from the Jason-1, 2 and 3 missions from January 2002 to December 2019, allows the analysis of the decadal evolution of coastal sea level and fills the coastal gap where sparse sea level information is currently available.

¹LEGOS, 18 Avenue Edouard Belin, Toulouse Cedex 9 31401, France. ²Technical University of Munich, Arcisstrasse 21, Munich 80333, Germany. ³National Oceanography Centre, 6 Brownlow Street, Liverpool L3 5DA, UK. ⁴SKYMAT Ltd., 11 Cedar Crescent, Southampton SO52 9FU, UK. ⁵CLS, Rue Hermes, Ramonville-Saint-Agne 31520, France. ⁶SERCO/ESRIN, Largo Galileo Galilei 1, Frascati 000-44, Italy. ⁷European Space Agency (ESA-ESRIN), Largo Galileo Galilei 1, Frascati 000-44, Italy. ✉email: anny.cazenave@legos.obs-mip.fr

The successive high-precision altimetry missions launched during the past three decades have not only revealed that the global mean sea level is rising at a mean rate of 3.3 ± 0.4 mm/yr^{1,2} but is also accelerating³. Their near-global coverage reveals that the rate of sea level rise is not uniform⁴, with some regions experiencing higher rate than the global mean by a factor of two to three. The causes of the global mean rise and acceleration, as well as of the changes observed at regional scale, are now well understood and quantified^{1,2,5}. At global scale and over the altimetry era (since 1993), thermal expansion of sea waters and land ice melt induced by anthropogenic global warming, explain respectively 40% and 55% of the sea level rise^{1,2}. At regional scale, non-uniform distribution of the ocean heat content remains the main cause of sea level rise⁴.

At the coast, the rate of sea level change on interannual to decadal time scales, results from the superposition of the global mean, the regional variability, plus a local contribution related to processes specific to near-shore areas⁶. The latter operate over a broad range of time scales, including interannual to multi-decadal time scales (the focus of the present study). For example, natural climate modes, such as ENSO (El Niño Southern Oscillation) and IOD (Indian Ocean Dipole), induce eastward propagating equatorial Kelvin waves affecting coastlines in the equatorial Pacific and Indian oceans^{6,7}. In the Atlantic Ocean, links between the NAO (North Atlantic Oscillation) and coastal sea level have been reported although the exact acting mechanisms remain unclear⁶. Changes in coastal sea level may also result from changes in coastal currents, driven by bathymetry and shape of coastal boundaries, and changing forcing factors, e.g., trend in wind stress. Fresh water discharge to the coastal ocean delivered by rivers in deltas and estuaries is another process able to produce sea level variations at the coast though water mass and density changes⁸. Wind-generated waves caused by changes in atmospheric circulation induced by anthropogenic climate change can also play a significant role in changing sea level very close to the coast⁹. Such coastal processes may not only directly change coastal sea level, but also mediate the coastal response to open-ocean forcing.

Due to all the involved processes, coastal sea level may greatly vary from one location to the other. Characterizing this spatial variability is crucial to understanding how coastal sea level varies on interannual to multidecadal time scales. Yet, this remains a key scientific challenge due to the lack of systematic coastal observations. Furthermore, sea level projections for the future decades¹ do not account for small-scale coastal processes, a major source of uncertainty and limitation for coastal communities and

adaptation purposes. Improved spatial coverage of sea level measurements in coastal areas would represent a first major step to progress. This would contribute to answering the important question: “Is coastal sea level rising at the same rate as in the open ocean?”¹⁰. Historical tide gauges provide invaluable information on coastal sea level change relative to the ground (the quantity of interest for coastal populations). However, long-term tide gauge records are mostly available for mid-latitude regions of the northern hemisphere. Although satellite altimetry only provides absolute sea level change in a geocentric reference frame (unlike tide gauges, altimetry does not measure vertical land motions), this technique allows to estimate climate-related coastal sea level changes with an extended coverage. Hence both tide gauges and altimetry can be considered as fully complementary.

As an extension of the Climate Change Initiative (CCI) Sea Level Project supported by the European Space Agency (ESA), dedicated to produce an improved altimetry-based global sea level product¹¹, we performed a regional reprocessing of altimetry data of the Jason-1, Jason-2 and Jason-3 altimetry missions (see <https://www.jpl.nasa.gov/missions/jason-3/> and <https://www.avisio.altimetry.fr/> for a detailed description of these missions) to extend the spatial coverage of sea level data as close as possible to the coasts. The study regions include North and South America, Northeast Atlantic, Mediterranean Sea, Africa, North Indian Ocean, Asia and Australia. Figure 1 shows the areas (red polygons) where the regional reprocessing has been implemented. However, in the following we will focus on the coastal zones only, i.e., on the satellite track portions starting from 20 km in the open ocean towards the coast.

Results

Altimetry data reprocessing. The present reprocessing has first consisted of re-computing altimeter ranges (i.e., altitude of the satellite above the sea surface) from along-track, high-resolution (20 Hz, i.e., 300 m resolution) altimetry data of the successive missions Jason-1, 2 and 3 in order to cover the January 2002 to December 2019 (18-year long) time span. It has been done with the Adaptive Leading-Edge Subwaveform (ALES) retracking method¹², designed for improving altimetry measurements in the coastal zone (while also suitable for the open ocean). The ALES retracking also retrieves one of the geophysical corrections applied to the range measurements, the so-called sea state bias, that depends on the significant wave height, also derived from the radar echoes¹³. Additional post-processing^{14–16} have consisted of applying adapted geophysical and environmental corrections for

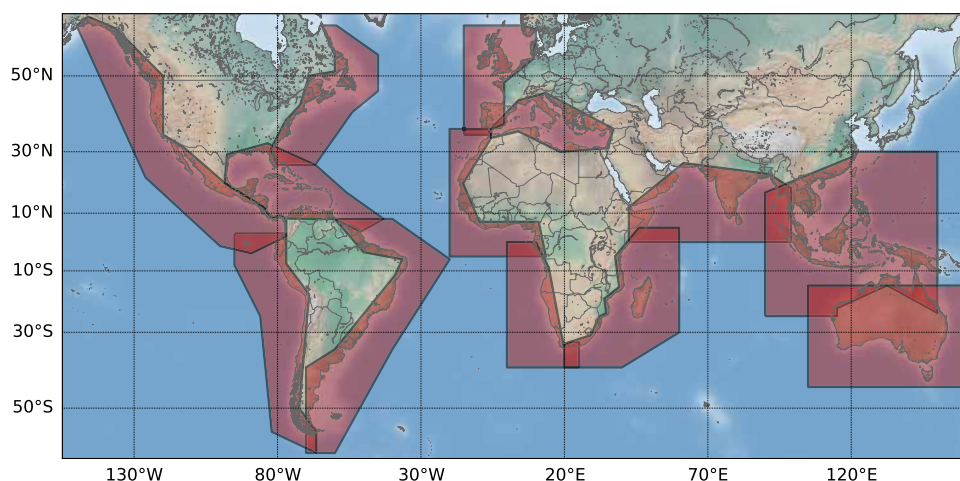


Fig. 1 Map of the studied coastal regions. Polygons (in red) represent the areas where the satellite data reprocessing has been implemented.

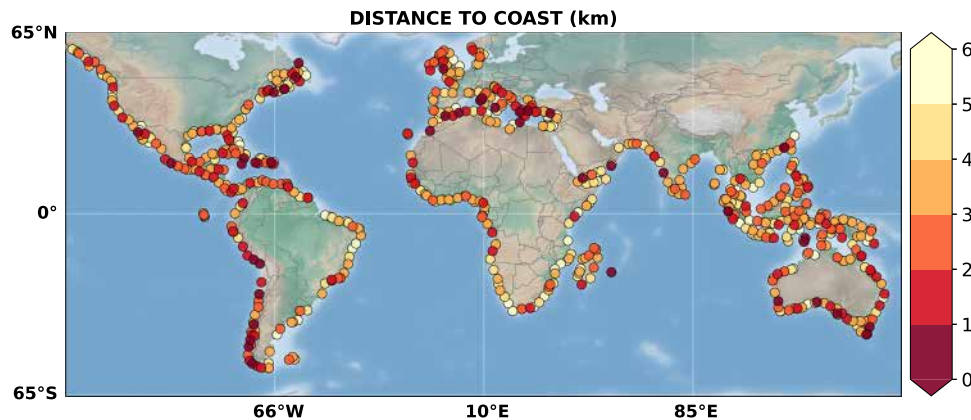


Fig. 2 Distance to coast of the 756 virtual coastal stations. Dots represent the location of the virtual coastal stations and associated colors indicate the closest distance (km) to the coast reached by the first valid point along the Jason tracks.

the coastal zones, re-estimating the inter-bias missions at a regional scale, and applying a dedicated editing in order to eliminate noisy data. Finally, only the near-shore sea level data, target of this study, are selected. The processing methodology is described in the Method section (it summarizes a more detailed description¹⁷ of the processing applied to a previous version of the data over a shorter time span and reduced geographical coverage). A previous version of this data set was recently validated against tide gauge measurements¹⁷ (see Methods). This reprocessing provides monthly sea level anomaly time series and associated trends computed over the 18-yr time span along the Jason tracks, from 20 km offshore towards the coast, with an along-track resolution of 300 m.

Virtual coastal altimetry stations. The closest distance to the coast of the first valid point along the track defines a “virtual” coastal station. Our comprehensive data editing procedure (see Methods) has led to the selection of 756 virtual stations, all located within 6 km to the coast (see Fig. 2; virtual stations further than 6 km have not been selected). The motivation for the 6 km threshold, relatively close to the coast, is to assess whether the observed coastal trends are similar to what is observed offshore, as we now benefit from this reprocessing that provides valid sea level data very close to the coast. Note that our reprocessing also provides sea level anomalies and trends as far as 20 km from the coast (see Data Availability section). While in the present study we focus on the 756 satellite track portions on which the first valid point is located at less than 6 km from the coast, we intend in the near future to expand our data set with additional track portions where the virtual station is located between 6 and 10 km. This will increase by 150 the number of virtual stations. Thus, the concept of virtual stations is clearly dependent of a given dataset.

Figure 3 shows a histogram of the closest distance to coast distribution with this 6 km cutoff. Among these 756 virtual coastal stations, 271 are located at less than 3.5 km from the coast (with several of them as close as 1 km or less from the coast). On average, the closest distance to the coast with valid sea level anomalies and trends is 3.5 km.

In Fig. 4 are presented three examples of along-track sea level trends against distance to the coast (one with trend almost constant, two with increasing/decreasing trends in the last 5 km towards the coast).

Coastal trends versus regional trends. In Fig. 5 are presented coastal sea level trends at virtual stations located at less than 3.5 km from the coast (cut-off chosen here for visibility).

Coastal sea level trends shown in Fig. 5 are averaged over 2 km along-track, using the closest available data to the coastline. The regional sea level trends derived from a $\frac{1}{4}^\circ$ resolution gridded altimetry product, are shown in the background. They are also computed over January 2002 to December 2019 using the Copernicus Climate Change Service product (C3S, version DT2021, <https://climate.copernicus.eu>).

From Fig. 5, we visually note that in some regions, trends at the virtual stations differ from the regional background. This is particularly obvious in the southeast Asian region where the coastal trends are lower than regional open ocean trends. One may invoke different processing approaches between the C3S gridded product and our high-resolution dataset. The C3S product has benefitted from orbit error reduction via a global adjustment of ascending and descending satellite tracks and results of an optimal interpolation. But the orbit error is of very long wavelength (>1000 km) and cannot explain the differences we observe in some coastal zones between sea level trends at 15 km offshore and within the last 4–5 km to the coast. Moreover, the C3S product is based on 1-Hz (~ 5 –6 km resolution) altimetry data, therefore any high-resolution information will be missed, without counting on the smoothing effect of the optimal interpolation and the data gaps (of several tens of km) between the satellite tracks.

We systematically compared coastal trends with offshore trends (assumed here at the average distance 15–17 km from the coast along the available track portion), and found no difference (within ± 2 mm/yr, i.e., of the maximum level of trend uncertainties) at 78% of the 756 virtual stations. In the remaining 22%, we observe either a smooth trend increase (7%) or decrease (15%) in the last ~ 4 –5 km to the coast (examples are shown in Fig. 4). Figure 6 displays the coastal trend behavior depending on regions.

Although it had been expected that coastal processes (e.g., coastal currents, wind & waves, fresh water input in river estuaries) may cause significant near-shore departure in coastal sea level trends from open ocean trends, the results presented here do not depict such effects at 78% of the selected sites. However, at a few sites, we observe a larger or smaller trend close to the coast compared to offshore, with a significant increase or decrease of a few mm/yr (i.e., larger than the trend uncertainty). In Ref. 18, we investigated in much details all sources of processing errors (retracking procedure, geophysical corrections applied to the data, etc.) potentially able to cause the change in sea level trend close to the coast and concluded that none could explain the observed trend behavior, suggesting rather a physical process effect. It is also worth noting that in all reported coastal

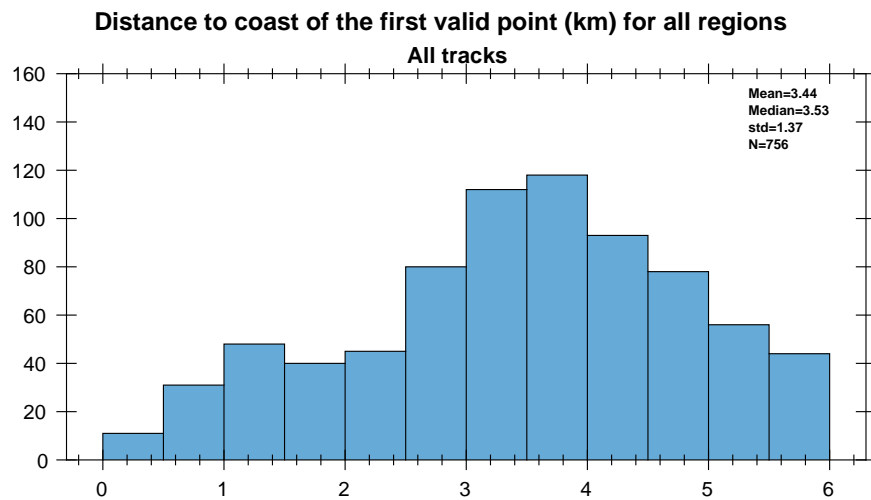


Fig. 3 Distribution of the distance to the coast of the 756 virtual stations. As shown by this histogram, the median value of the closest distance to the coast is about 3.5 km.

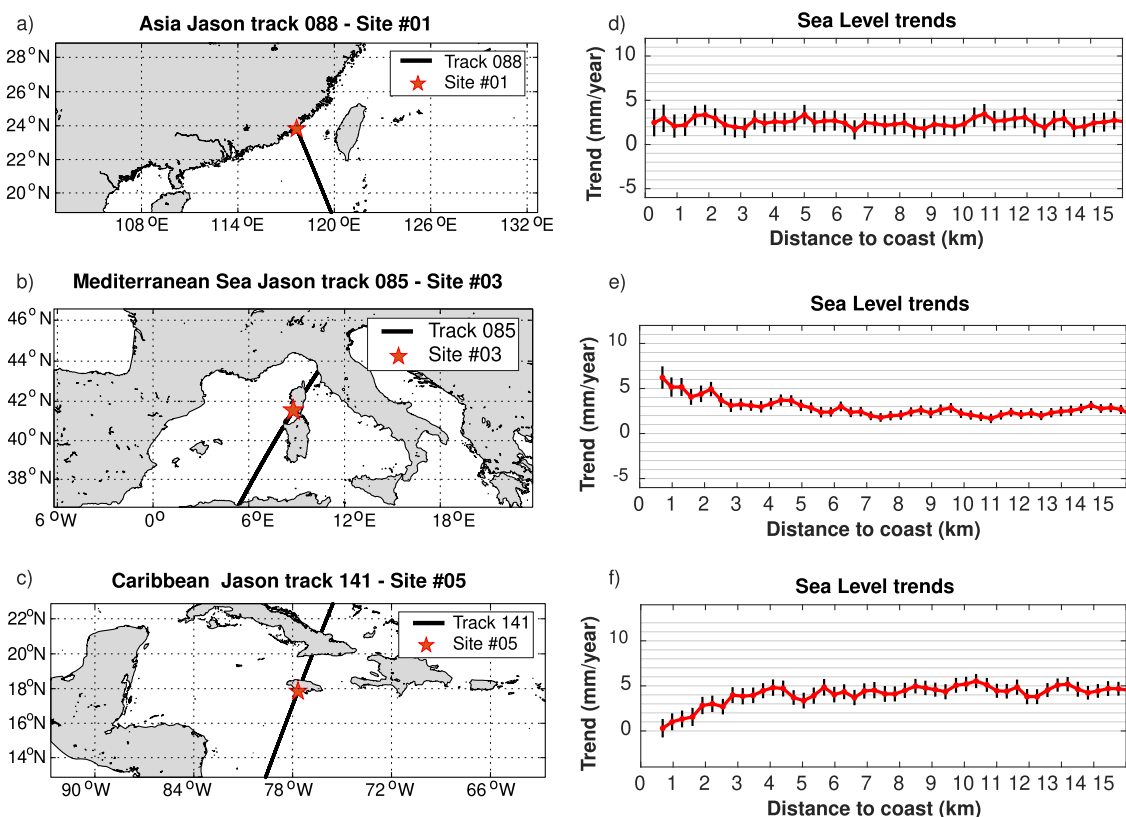


Fig. 4 Examples of along-track sea level trends and associated 1-sigma error against distance to the coast. **a–c** show coastal site location (red star) and associated Jason track (black line). **d–f** represent sea level trends against distance to the coast (red curve) and associated trend error (black vertical bar).

trend departures compared to offshore (15–17 km away from the coast), the trend increase or decrease is continuous along the track, with no discontinuity from one point to another.

Over the study period, we note that decreasing coastal trends dominate. This is especially the case in the Asian region and around Australia. Small-scale coastal processes may be responsible for such a behavior as discussed above. Figure 7 shows the distribution of virtual stations closer than 3.5 km to the coast, for which the coastal trend differs by more than 2 mm/yr in the last 4–5 km to the coast compared to offshore (here assumed at 15–17 km).

From Fig. 7, we do not see any concentration of trend departures from offshore trends in a particular region. All studied coastlines are concerned.

Discussion

The new altimetry-based coastal sea level data set presented here fills for the first time a spatial data gap along large portions of the world coastlines. It provides an unprecedented coastal coverage for any long-term altimetry data set. It also provides considerably refined information designed for climate applications, compared

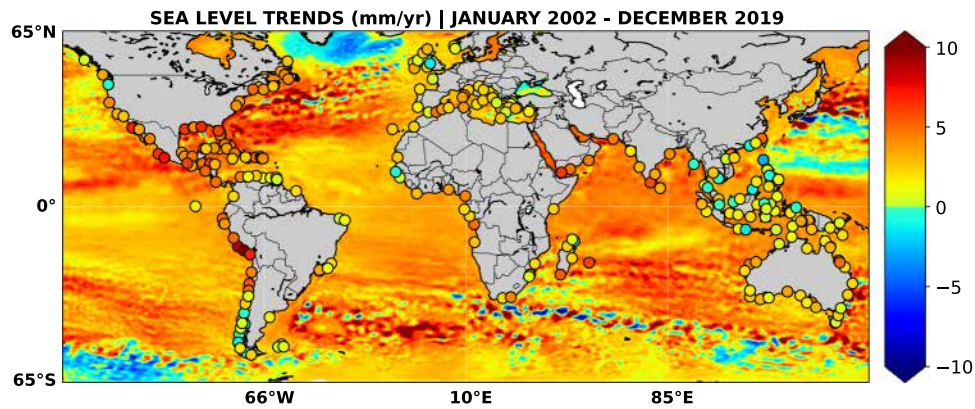


Fig. 5 Coastal and regional sea level trends (mm/yr) over the 18-yr time span. Coastal trends at virtual stations closer than 3.5 km from the coast are indicated by the black circles. The background map shows regional sea level trends from the C3S data set.

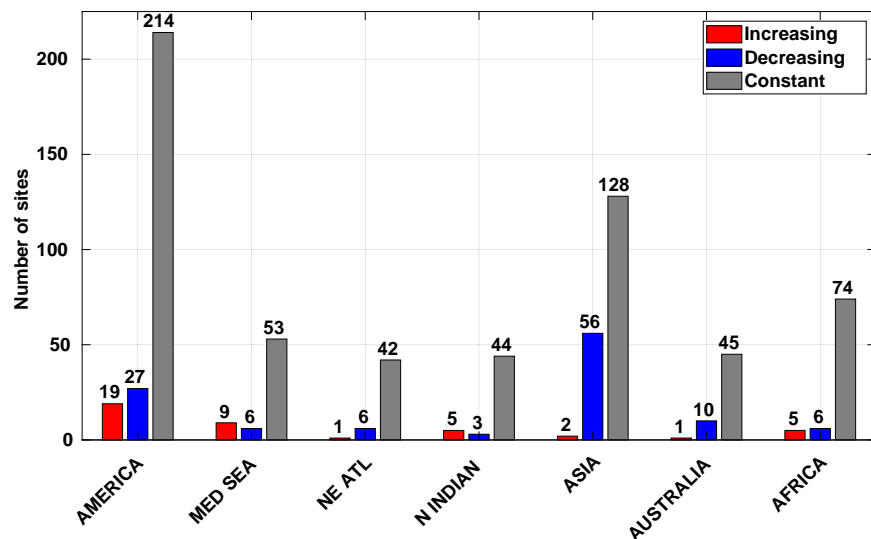


Fig. 6 Statistics of coastal trend behavior at the 756 virtual stations compared to 15-17 km offshore. Gray, red, and blue bars correspond to constant, increasing and decreasing coastal trends, respectively, depending on regions (America, Mediterranean Sea, Northeast Atlantic, North Indian Ocean, Asia, Australia, Africa).

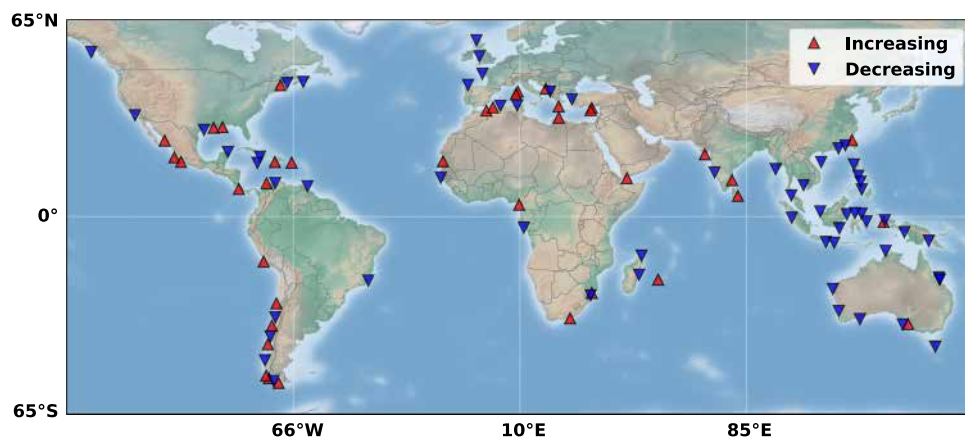


Fig. 7 Virtual stations located at less than 3.5 km from the coast where the coastal trend is different from offshore. Red and blue triangles correspond to increasing and decreasing trends in the last ~4-5 km towards the coast compared to offshore (assumed here 15-17 km away) (as illustrated by the examples shown in the middle and bottom panels of Fig. 4).

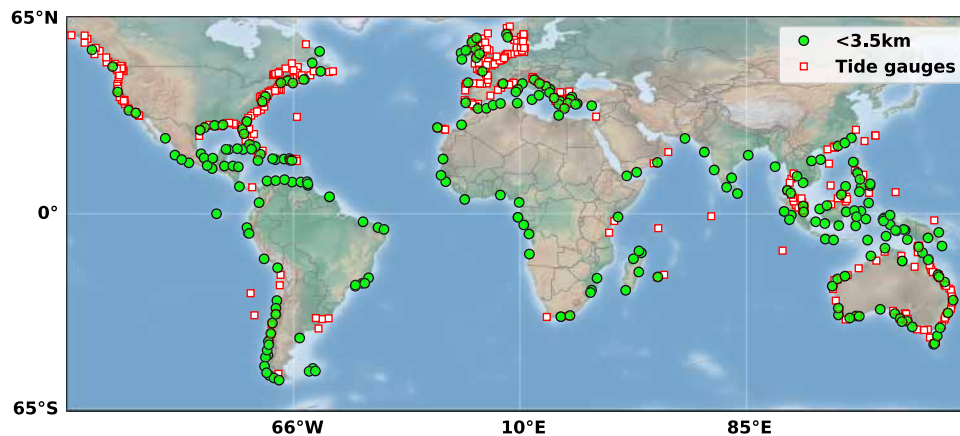


Fig. 8 Network of 271 virtual coastal stations located within 3.5 km from the coast (green dots). Red/white squares correspond to tide gauges having monthly data over January 2002–December 2019 (with only 24 months of missing data; 400 sites) (tide gauge data are downloaded from the Permanent Service for Mean Sea level²⁵).

with currently available global multi-mission gridded altimetry-based sea level products (e.g., from the Copernicus Marine and Climate services; <https://marine.copernicus.eu>; <https://cds.climate.copernicus.eu/cdsapp#!/dataset/satellite-sea-level-global>) that cover the coastal areas only with a $\frac{1}{4}^\circ$ spatial resolution (in reality, not better than 100 km considering the inter-track spacing of existing missions¹⁹) and use 1-Hz (~ 5 km resolution) altimetry data. We have introduced the new concept of virtual coastal stations that will complement the current network of tide gauges (although satellite altimetry only provides absolute sea level measurements in a geocentric reference frame, unlike tide gauges that measure sea level relative to the ground, hence are sensitive to vertical land motions). This new set of virtual stations is the coastal ocean counterpart of virtual altimetry stations in ungauged river basins on land, defined as the intersection of the river with the satellite track, which routinely provide multidecade-long water level time series (e.g., <https://hydroweb.theia-land.fr/>). The network of virtual coastal stations proposed here should be of invaluable interest for estimating present-day (absolute) sea level rise along the world coastlines, especially in regions devoid of in situ tide gauges. To illustrate this, Fig. 8 shows the distribution of the 271 virtual stations located within 3.5 km from the coast and of current tide gauges that have monthly sea level data over the study time span (with not more than 24 months of missing data).

While in North America, Western Europe and Australia, the tide gauge coverage is very good, this is not the case in several other regions, e.g., in Central America, part of South America, Africa and North Indian Ocean. Although here we are only able to provide reprocessed coastal sea level data along the Jason tracks, this new data set will offer new insights on how sea level trends evolve spatially along the world coastlines, in particular in regions lacking tide gauges. It is worth noting that the track coverage of current and planned altimetry missions will not permit, in any event, to reach an inter-track resolution of 300 m, similar to this study's along-track resolution, hence to produce a very high-resolution gridded coastal sea level data set.

We have seen that at 78% of the virtual stations, the coastal sea level trend is similar to the offshore trend. An interesting outcome of this result is the possibility of extrapolating sea level trends up to the coast at these specific locations, using standard gridded data sets. Since the latter cover the whole altimetry era (January 1993 to present), longer time series of coastal sea level trends can be estimated at these sites. For the remaining 22% sites, the trend behavior close to the coast has been found different from offshore. A recent study by Harvey et al.²⁰

compared altimeter trends (from a classical gridded product²¹) at the nearest point from a tide gauge site (tide gauge records corrected for vertical land motions–VLM–) along the western and eastern coasts of North America, and found general poor agreement (see their Fig. 8a). The authors suggest that VLM uncertainties could explain the large spread they observe. But another possibility may be invoked: the offshore versus coastal trend differences could also be due to small-scale processes acting in the close vicinity of the coast (hence not seen by the low-resolution gridded altimetry product).

Investigating small-scale coastal processes is clearly an important research goal to pursue; an objective well beyond the scope of the present study. In effect, the general lack of in situ coastal data on ocean dynamics, as well as of high-resolution ocean models (grid mesh smaller than 1 km) prevents from any systematic quantification of coastal phenomena causing the reported trend increase or decrease nearby the coast. Our previous investigations^{18,22} at one of such virtual station (Senetosa, South Corsica, Mediterranean Sea; see Fig. 4 above) where a high-resolution (400 m) ocean model was available, suggested that the observed trend increase in the last ~ 4 –5 km towards the coast could be explained by sea water temperature increase and salinity decrease, and associated coastal current change. However, no generalization can be made. Depending on the coastal morphology, bathymetry and shelf configuration, presence of a river estuary, atmospheric forcing, etc., small-scale coastal processes affecting sea level may differ from one site to another. Future efforts need to be devoted to this important goal, not only to improve our current understanding of present-day coastal sea level changes but also to improve climate models simulating future sea levels in highly-populated and vulnerable coastal regions of the world.

Methods

Sea level data from altimetry and tide gauges. We first considered Geophysical Data Records (GDRs) provided by AVISO + (<https://www.aviso.altimetry.fr/>) for the successive Jason-1 (from January 2002 to January 2009), Jason-2 (from July 2008 to September 2016) and Jason-3 (from February 2016 to December 2019) missions. Along the ground tracks, a single multi-mission time series at a near 10-day sampling (Jason orbital cycle), with a spatial resolution of ~ 0.3 km, is then computed using the method described below.

We also used gridded altimetry-based sea level time series from the Copernicus Climate Change Service (C3S, <https://climate.copernicus.eu>) over the same time span (January 2002 to December 2019) to compute regional (open ocean) sea level trends.

Tide gauges sites with valid data over January 2002 to December 2019 (with less than 24 months data missing) are from the Permanent Service for Mean Sea level (www.psmsl.org).

Retracking and computation of sea level anomalies. In a coastal zone band of ~20 km wide along the coastline, the radar signal reflected from the Earth surface within the satellite footprint is often corrupted by land contamination, leading to rejection of most sea level data in this domain. The percentage of valid altimetry-based sea level data is around 90% in the open ocean but it regularly drops to less than 10% from 20 km offshore towards the coast (Fig. 1 of Ref. 17). The loss of valid sea level data in the coastal zone is caused by land contamination with the radar footprint, leading to distorted waveforms (i.e., magnitude and shape of the radar echo after reflection on the Earth's surface), compared to the classical step-like waveforms over the open ocean. To retrieve valid radar range data in the coastal zones, we applied the Adaptive Leading-Edge Subwaveform (ALES) retracker¹² to 10-day, along-track, 20 Hz (300 m resolution) radar echoes of the Jason-1, 2 and 3 missions, over January 2002 to December 2019. ALES observations have the

advantage of increasing the quality and quantity of altimeter range retrievals in the coastal zone without affecting the open ocean performances. In particular, in terms of precision in the open ocean, Smith et al. (Ref. 23) demonstrated that the power spectra of sea level data computed with ALES shows the lowest noise among all available retrackers, for spatial scales of variability in the range 10–50 km. The larger noise level at smaller scales (due to the smaller portion of the waveform considered in the retracking process) is compensated by the application of the sea state bias at 20-Hz. In effect, Passaro et al. (Ref. 13) showed that the altimeter ranges from ALES, when corrected for sea state bias using the estimations of wave and wind speed from the same retracker at 20-Hz (as in this study), are more precise than the current baseline for the Jason products (based on the classical MLE3 or MLE4 retracks with sea state bias correction at 1-Hz; <https://aviso.altimetry.fr>). Considering as an example the area of the North Sea, the authors¹³ showed that the configuration with ALES achieved a precision (based on sea level differences at crossover points between ascending and descending satellite tracks) of about 0.07 m against about 0.09 m for the standard product, for a significant wave height of 2 m.

In this study, the altimeter range values retracked with ALES were further combined within the X-TRACK processing system developed at the LEGOS (Laboratoire d'Études en Géophysique et Océanographie Spatiales) laboratory¹⁴, to obtain 20-Hz geophysically-corrected sea surface height times series along the satellite tracks. The geophysical corrections applied to the retracked data are listed in Ref. 17. A first validation was applied, consisting of analysing the behavior of the applied geophysical corrections, then editing and recomputing the suspicious corrections in order to maximize the number of near-shore valid data^{14,15}. The corrected sea surface heights of each satellite orbital cycle were further projected onto fixed points along a nominal ground track (defined as the barycenters of 20-Hz along-track data obtained from one cycle to another). These sea surface heights were further converted into sea level anomalies by subtracting a precise regional mean sea surface (computed by inversion of all the available corrected sea surface height data along the ground tracks^{14,15}). The sea level anomalies at 10-day interval (the temporal resolution of the Jason altimetry data) were further averaged on a monthly basis. The corresponding data set consists of along-track, high resolution (~300 m) monthly sea level anomaly time series covering the coastal zones of the study regions (Fig. 1) from 20 km offshore to the coast. However, as the distance to the coast decreases, the retracked data are in general more noisy. Another editing based on the sea level trends has been applied that led us to delete dubious data in the close vicinity of the coast (see criteria below). Depending on the region, this additional editing has resulted in a variable closest distance to the coast to be reached, with an average value of 3.5 km. Compared to the current resolution of existing altimetry products (>100 km¹⁹), this is a significant progress.

Distribution of coastal and offshore sea level trend errors

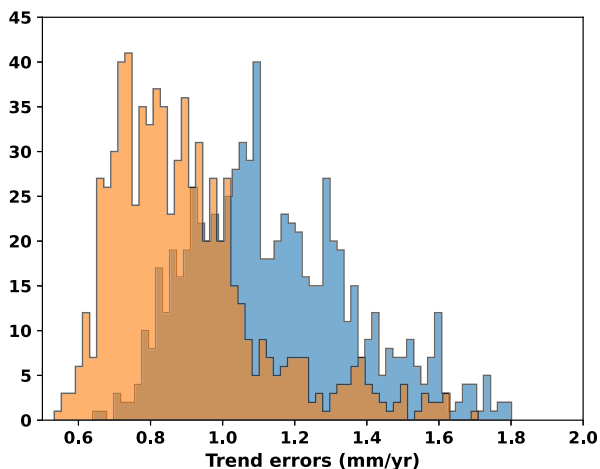


Fig. 9 Distribution of coastal (blue bars) and offshore (orange bars) trend errors (in mm/yr). The histograms show that the coastal trend errors are slightly higher, on average, than offshore trend errors.

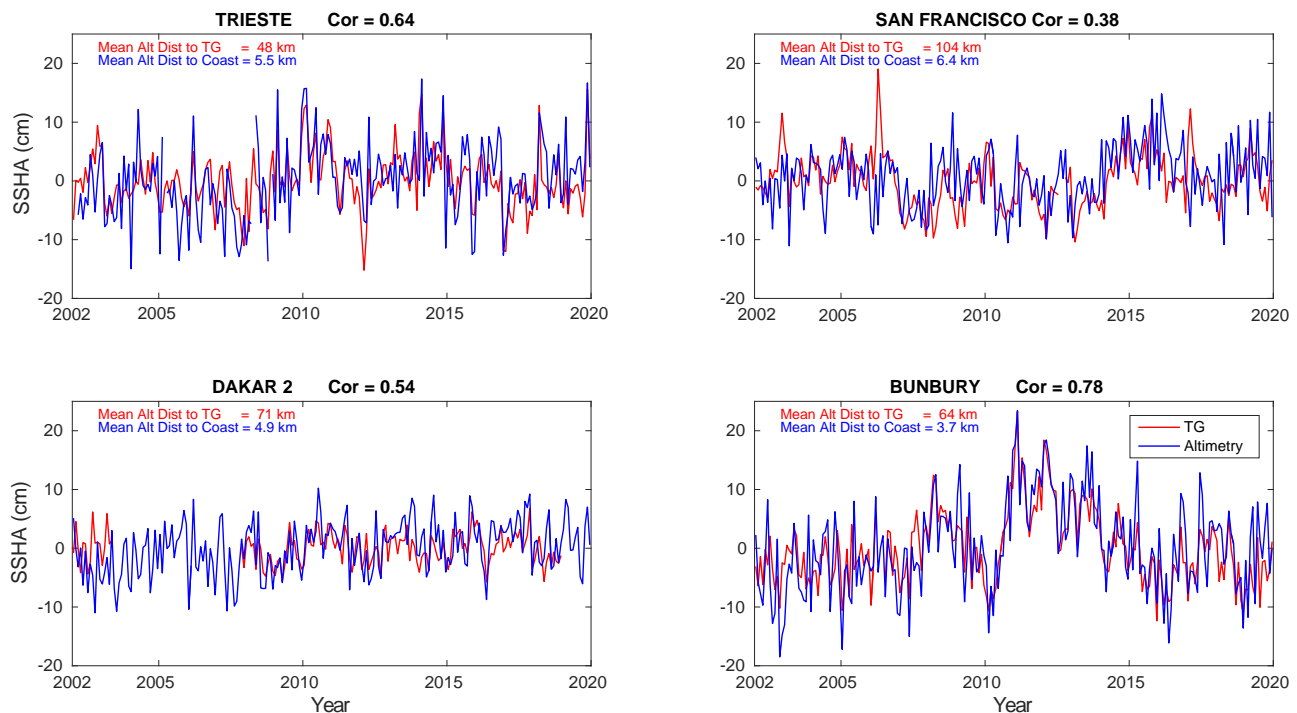


Fig. 10 Tide gauge (TG, red curve) and altimetry (Alt, blue curve) comparison at four selected sites, Trieste (Mediterranean Sea), San Francisco (North America), Dakar 2 (West Africa) and Bunbury (Australia). Each tide gauge location shows the correlation and time series between the closest averaged altimeter track and the tide gauge. The mean distance of the altimetry observations to both the tide gauge and the coast is also shown. SSHA means sea surface height anomaly.

Linear trends and uncertainty estimations. To compute along-track sea level trends over the 18-yr long study period, we first removed the annual and semi-annual cycles and applied a strict selection procedure, using the following criteria: (1) at least 75% of valid data for each 20-Hz sea level anomaly time series; (2) distribution of the valid data as uniform as possible though time—in a number of cases, Jason-1 data were missing, thus the corresponding sea level time series was discarded; (3) trend values in the range -15 mm/yr to $+15$ mm/yr; this threshold is based on spurious discontinuities sometimes observed in sea level trends from one point to another; (4) standard trend errors < 2 mm/yr; (5) continuity of trend values between successive 20-Hz points; too abrupt changes in trends over very short distances were considered as spurious. Statistics performed on the standard trend errors against distance to the coast showed that the mean trend error at the closest points to the coast is 1.15 mm/yr compared to 0.9 mm/yr for offshore trends. Figure 9 shows the distribution of coastal and offshore trend errors. In all cases, if the trend error is > 2 mm/yr, whatever the point position along the track, the data are discarded.

The uncertainty on the trend estimate is the classical 1-sigma standard error of the least-squares fit. More realistic error estimates should be worth to be addressed in the future, on a case-by-case approach. This is beyond the scope of the present study.

Validation with tide gauges. A previous version of the coastal sea-level product was recently validated against tide gauge observations in Ref. 17, and we defer to that study for full details. Here, we briefly summarize the results of such validation. To ensure a proper validation, tide gauge records were adjusted for vertical land motions using Global Positioning System (GPS) vertical velocities. We found an average correlation of 0.5 between monthly tide gauge records and point-level altimetry data, but the correlation increases to 0.78 when averaging the altimetry data along and across tracks for data that fall within a small distance from each tide gauge. The increase in correlation achieved by averaging occurs because it reduces both sampling uncertainty (monthly means are based on more than 3 values) and the influence of small-scale variability. Linear trends were found to be in good statistical agreement at 64% of the tide gauge stations.

As additional validation, here we compare time series of sea level at four tide gauge sites with data from their closest altimetry track (Fig. 10). Both the tide gauge and altimeter observations had the annual and semi-annual cycles and trend removed. To reduce the effect of small-scale errors on the altimeter observations, we averaged the 10 points closest to the coast along the altimeter track (data that fall within ~ 5 km of the coast). The correlation between tide gauge and altimetry observations gives an insight into how altimetry observations can represent sea level variability close to the coast (~ 5 km). The site with the highest correlation is Bunbury (0.78) while the lowest correlation (0.38) is found at San Francisco (0.38). Each tide gauge location has unique sea-level properties as illustrated by the range of amplitude of the sea-level variability between sites. Differences in correlation between sites largely reflect differences in the length scales of the sea-level signals typical of each site: shorter length scale magnify differences between altimetry and tide gauges due to spatial separation.

Data availability

The data set (version v2.1) is freely available on the SEANOE repository: <https://doi.org/10.17882/74354>. It provides monthly sea level anomalies time series and associated sea level trends computed over January 2002 to December 2019 at points located along 756 satellite track portions from 20 km offshore to the coast, with an along-track resolution of 300 m. The SEANOE web page also gives access to the Product User Guide that describes the various variables associated with the data set. Temporal extension of the coastal sea level time series along the Jason tracks is planned on the short term.

Code availability

The operational X-TRACK system has been fully described in refs. 14,15. All other post-processing codes are available on demand to the authors. All figures were produced by the authors. The maps and all the figures were created with the MATLAB and PYTHON softwares. We also used the Global Self-consistent, Hierarchical, High-resolution Geography Database (GSHHG)²⁴ as third-party data to draw continental coastlines in Figs. 1, 2, 4, 5, 7 and 8.

Received: 15 December 2021; Accepted: 29 April 2022;

Published online: 16 May 2022

References

1. IPCC, 2019. Special Report on the Ocean and Cryosphere in a Changing Climate [H.-O. Pörtner, et al. (eds.)].

2. Horwath, M. et al. Global sea level budget and ocean mass budget, with focus on advanced data products and uncertainty characterization. *Earth Syst. Sci. Data* **14**, 411–447 (2022).
3. Dieng H., Cazenave A., Meyssignac B. and Ablain M., New estimate of the current rate of sea level rise from a sea level budget approach, *Geophys. Res. Lett.*, **44**, <https://doi.org/10.1002/2017GL073308>, 2017.
4. Hamlington B. et al., Understanding of contemporary regional sea-level change and the implications for the future, *Rev. Geophys.* <https://doi.org/10.1029/2019RG000672>, 2020.
5. The WCRP Global Sea Level Budget Group, Global sea level budget. 1993–present. *Earth Syst. Sci. Data* **10**, 1551–1590 (2018).
6. Woodworth, P. L. et al. Forcing factors affecting sea level changes at the coast. *Surveys Geophys.* **40**, 1351–1397 (2019).
7. Han, W. et al. Impacts of basin-scale climate modes on coastal sea level; A review. *Surveys Geophys.* **40**, 247–296 (2019).
8. Durand, F. et al. Impact of continental freshwater runoff on coastal sea level. *Surveys Geophys.* **40**, 1437–1466 (2019).
9. Dodet, G. et al. The contribution of wind-generated waves to coastal sea level changes. *Surveys Geophys.* **40**, 1563–1601 (2019).
10. Vignudelli, S. et al., Satellite altimetry measurements of sea level in the coastal zone. *Surveys Geophys.* <https://doi.org/10.1007/s10712-019-09569-1>, 2019.
11. Legeais, J. F. et al. An improved and homogeneous altimeter sea level record from the ESA Climate Change Initiative. *Earth Syst. Sci. Data* **10**, 281–301 (2018).
12. Passaro, M. et al. ALES: A multi-mission adaptive subwaveform retracker for coastal and open ocean altimetry. *Remote Sens. Environ.* **145**, 173–189 (2014).
13. Passaro, M., Nadzir, Z. A. & Quartly, G. D. Improving the precision of sea level data from satellite altimetry with high-frequency and regional sea state bias corrections. *Remote Sensing Environ.* **218**, 245–254 (2018).
14. Birol, F. et al. Coastal applications from nadir altimetry: example of the X-TRACK regional products. *Adv. Space Res.* **59**, 936–953 (2017).
15. Birol, F. et al. The X-TRACK/ALES multi-mission processing system: new advances in altimetry towards the coast. *Adv. Space Res.* **67**, 68 (2021).
16. Marti, F. et al. Altimetry-based sea level trends along the coasts of western Africa. *Adv. Space Res.* **68**, 504–522 (2021).
17. Benveniste, J. et al. Coastal sea level anomalies and associated trends from Jason satellite altimetry over 2002–2018. *Nat. Sci. Data* **7**, 357 (2020).
18. Gouzenes, Y. et al. Coastal sea level change at Senetosa (Corsica) during the Jason altimetry missions. *Ocean Sci.* **16**, 1–18 (2020).
19. Ballarota, M. et al. On the resolutions of ocean altimetry maps. *Ocean Sci.* **15**, 1091–1109 (2019).
20. Harvey, T. C. et al. Ocean mass, steric dynamic effects, and vertical land motion largely explain US coast relative sea level rise. *Commun. Earth Environ.* **2**, 223 (2021).
21. Zlotnicki, V. et al., MEASUREs gridded sea surface height anomalies version 1812. <https://doi.org/10.5067/SLREFCDRV2> (2019).
22. Dieng H. B., Cazenave A., Gouzenes Y. and Sow B. A., Trends and inter-annual variability of coastal sea level in the Mediterranean Sea: Validation of high-resolution altimetry using tide gauges and models, published online June 2021, *Adv. Space Res.* <https://doi.org/10.1016/j.asr.2021.06.022>, 2021.
23. Smith W. H. F. et al. Covariant errors in ocean retracers evaluated using along-track cross-spectra. OSTST (Ocean Surface Topography Science Team) (Meeting, Miami, USA, 2017).
24. Wessel, P. & Smith, W. H. F. A global, self-consistent, hierarchical, high-resolution shoreline database. *J. Geophys. Res.* **101**, 8741–8743 (1996).
25. Holgate, S. J. et al. New data systems and products at the Permanent Service for Mean Sea Level. *J. Coastal Res.* **29**, 493–504 (2013).

Acknowledgements

We gratefully acknowledge funding for this work: The European Space Agency supported the two phases of the Climate Change Initiative (CCI) for Sea Level and the CCI + phase for Coastal Sea Level, which has provided the majority of the support leading to the outcomes herein described, in addition to the specific grant reference 4000126561/19/I-NB for Yvan Gouzenes.

Author contributions

All authors contributed to parts of the research and analysis. AC coordinated the study. YG performed the coastal trend analyses and produced the Figs. 2, 3, 4, 5, 6, 7, 8 and 9. FL and AS produced Figs. 1 and 10 respectively. MP provided the retracked altimetry ranges and sea state bias correction. The sea level anomaly processing was performed by FB, FL and FN. FC and AS carried out the tide gauge validation. All authors, including JFL, JO, MR and JB, contributed to the interpretation of the results and further writing of the paper.

Competing interests

The authors declare no competing interests.

Additional information

Supplementary information The online version contains supplementary material available at <https://doi.org/10.1038/s43247-022-00448-z>.

Correspondence and requests for materials should be addressed to Anny Cazenave.

Peer review information *Communications Earth & Environment* thanks Marijan Grgic and the other, anonymous, reviewer(s) for their contribution to the peer review of this work. Primary Handling Editor: Heike Langenberg. Peer reviewer reports are available.

Reprints and permission information is available at <http://www.nature.com/reprints>

Publisher's note Springer Nature remains neutral with regard to jurisdictional claims in published maps and institutional affiliations.



Open Access This article is licensed under a Creative Commons Attribution 4.0 International License, which permits use, sharing, adaptation, distribution and reproduction in any medium or format, as long as you give appropriate credit to the original author(s) and the source, provide a link to the Creative Commons license, and indicate if changes were made. The images or other third party material in this article are included in the article's Creative Commons license, unless indicated otherwise in a credit line to the material. If material is not included in the article's Creative Commons license and your intended use is not permitted by statutory regulation or exceeds the permitted use, you will need to obtain permission directly from the copyright holder. To view a copy of this license, visit <http://creativecommons.org/licenses/by/4.0/>.

© The Author(s) 2022